Indian Journal of Geo Marine Sciences
Vol. 50 (08), August 2021, pp. 613-619

Comparing performance of inter-sensor NDVI for the detection of floating macroalgal blooms in the Yellow Sea

M H Sakib[a], A H A Rashid[b] & C-S Yang*[,c,d,e]

[a]Department of Agricultural Extension and Rural Development, Faculty of Agriculture, EXIM Bank Agricultural University Bangladesh, Chapainawabganj – 6300, Bangladesh

[b]Department of Aquatic Resource Management, Faculty of Fisheries, Sylhet Agricultural University, Sylhet – 3100, Bangladesh

[c]Marine Security and Safety Research Center, Korea Institute of Ocean Science & Technology, Busan – 49111, Korea

[d]Integrated Ocean Sciences, University of Science & Technology, Daejeon – 34113, Korea

[e]Department of Convergence Study on the Ocean Science and Technology, Ocean Science and Technology School, Korea Maritime and Ocean University, Busan – 49111, Korea

*[E-mail: yangcs@kiost.ac.kr]

Received 19 November 2019; revised 26 June 2021

There are many complains against macroalgal bloom (MAB) from all over the world for its high negative economic impacts. Early and precise detection of MAB occurance can reduce huge economic loss in tourism and marine business. Thus, this study aims to detect the MAB in the Yellow Sea (YS) by comparing performance of Normalized Difference Vegetation Index (NDVI) between Geostationary Ocean Color Imager (GOCI) and Landsat-8 sensors from 2014 to 2019. The largest MAB during this period was identified from Landsat-8 sensors along the coast of Sheyang and Qingdao of China in 2018. The locations of MABs were almost nearby areas during the begining phase of MABs in consecutive years. In successive years huge and dense MABs reached the brink of shoreline of Qingdao. In Landsat-8 images in most cases larger total areas of MABs were detected including very small pathches which could not be detected from GOCI due to low spatial resolution. The findings of this study will be helpful for scientists to choose between GOCI and Landsat-8 based on the objectives of their study.

[**Keywords**: GOCI, Landsat-8, MAB, Multispectral, NDVI, Yellow Sea]

Introduction

Massive growth of seaweed is called macroalgal bloom (MAB) which is being reported from the coastal regions in several seas[1-3]. Generally, the coastal eutrophication is the main reason for the rampant reproduction of large-scale seaweeds like *Ulva*[4-5]. During the last couple of years some vivid examples of such blooms were found in the Yellow Sea (YS) and in many other parts of the world[6-10]. Nowadays, MABs are being detected form satellite images by applying various vegetation indices. In 2008, large volume of macroalgae washed up on beaches close to Qingdao, and thus had the great negative aesthetic and amenity impacts on recreation, tourism, and marine installations of China[11-12]. Thereafter, it started to appear regularly in the central and southern regions of the YS[13]. Therefore, it is necessary to detect the macroalgae quickly and accurately in order to avoid hazards from their sudden beaching. For this purpose satellite data can be cost-effectively used to investigate large scale MABs[14-15]. In the last decade, hourly, monthly, and yearly distribution patterns of MABs were studied mainly by using images from several satellites like Geostationary Ocean Color Imager (GOCI)[16], Landsat-8, Himawari, Sentinel-1, Sentinel-2, etc. However, studies on detections of MABs with multisensors are scarce. Therefore, in this study GOCI and Landsat-8 are used together to compare their MAB detection capability in the YS.

In previous study some tiny portions of MABs in the YS could not be detected from GOCI images due to having a low spatial resolution (500 m)[16]. Therefore, high spatial resolution images from Landsat-8 (30 m) were also used in order to detect thin MAB patches. A popular vegetation index is Normalized Difference Vegetation Index (NDVI) for detecting floating macroalgae from satellite images[17]. In this study, NDVI is used accordingly to bring together the information about vegetation index profiles by using data from GOCI and Landsat-8. For some places in the YS GOCI data with corresponding Landsat-8 images were used to to observe variations of MAB pixels and patch (group of macroalgae pixels)

characteristics. Total areas of spatial distributions of MABs were also estimated from both satellite images.

Materials and Methods

Study area

Long-term occurrences of MABs in the YS area are investigated through this study. The mainland of China and Korea bounded a semi-enclosed basin of the northwest Pacific Ocean forming the YS (Fig. 1). It covers a wide area of around 417,000 km^2 and posseses a shallow basin (average depth 44 m)[18].

Methodology

In this study multispectral GOCI data were processed to generate NDVI images for detecting MABs[19]. GOCI covers an area of 2500×2500 km^2 centered on Korea, and its eight bands cover visible to near-infrared (NIR) spectral wavelengths. It gives daily earth observations data (8 times a day with hourly interval)[20]. The number of slots in GOCI is sixteen in which the YS covers the slots from 7 to 10[(ref. 18)]. GOCI data (level 2, ver. 2.0) were downloaded from the Korea Ocean Satellite Center (KOSC) website (http://kosc.kiost.ac.kr/eng/p10/kosc_p11.html) from 2014 to 2019[(ref. 21)]. By using the GOCI Data Processing System (GDPS), the satellite image data were transformed to Rayleigh corrected reflectance (Rrc) format which were further processed to NDVI by using the ENvironment for Visualizing Images (ENVI) softaware, version 4.7. For this purpose bands 5 and 8, were used.

Landsat-8 images were accessed from the Landsat archive at the US Geological Survey (USGS) website (https://earthexplorer.usgs.gov/)[22]. Images covering the YS in each year from April to September were first downloaded and then visually compared using respective true and false colour composite images (RGB band combinations 6, 4, 2, and 8, 4, 2, respectively for GOCI, and 4, 3, 2, and 5, 4, 3, respectively for Landsat-8). Finally six Landsat-8 images from May 2014 to August 2019 and respective dates' closest period clear GOCI images were used (Table 1). Preprocessing of Landsat-8 data to Rrc and then convertion to NDVI were directly done by using ACOLITE software[23].

The spectral characteristics of macroalgae in the YS in the visible and NIR bands are much alike that of the land vegetation; therefore most methods for monitoring macroalgae from optical satellite data are based on the "red edge" phenomenon of the vegetation spectrum which is the basis of NDVI[4,13]. The NDVI is calculated as:

$$\mathrm{NDVI} = \mathrm{NIR} - \mathrm{R} / \mathrm{NIR} + \mathrm{R}$$

Where, NIR and R denote Rrc in NIR and red bands, respectively. Image based threshold were used on NDVI for the extraction of macroalgae patches.

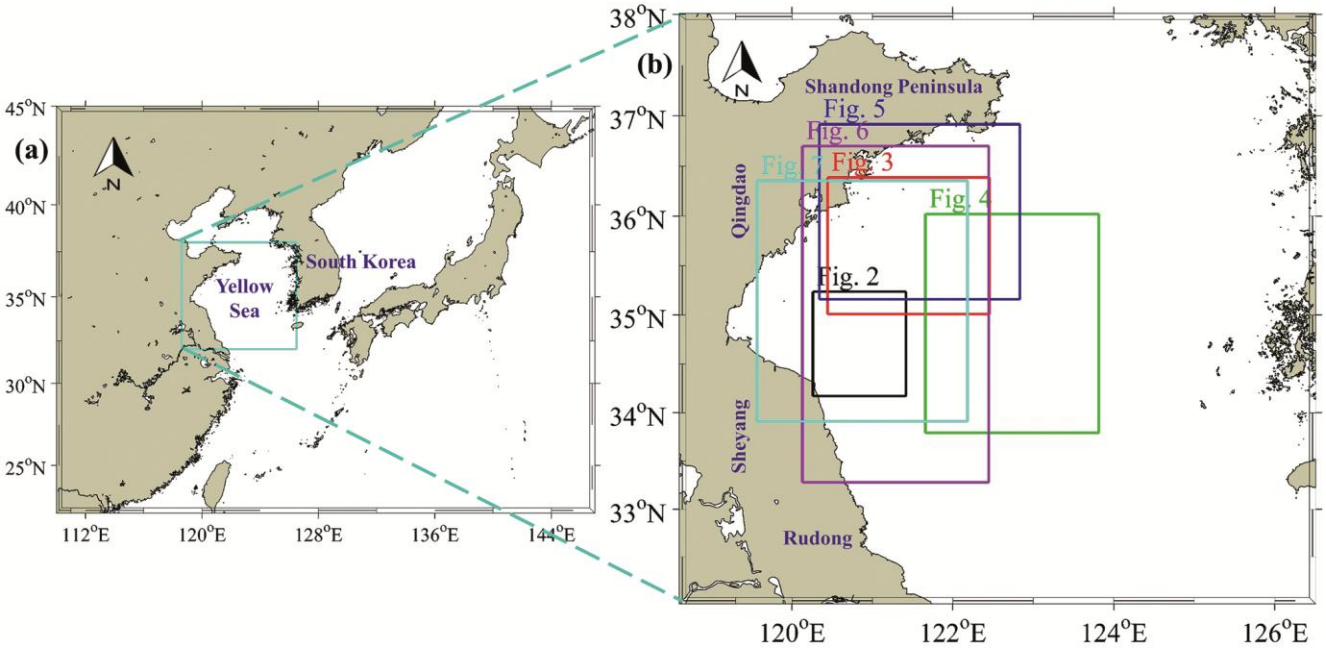

Fig. 1 — The study area in the Yellow Sea. The box of (a) is enlarged as the right map (b) where some rectangles shows the map areas for Figures 2 to 7

Table 1 — Landsat-8 and GOCI images used for this study

Satellite images	Path/row	Image date
LC08_L1TP_119036_20140519_20170422_01_T1	119/36	May 19, 2014
LC08_L1TP_119035_20150607_20180205_01_T1	119/35	June 07, 2015
LC08_L1GT_118036_20160618_20170323_01_T2	118/36	June 18, 2016
LC08_L1TP_119035_20170628_20170714_01_T1	119/35	June 28, 2017
LC08_L1GT_118036_20180624_20180704_01_T2	118/36	June 24, 2018
LC08_L1GT_118037_20180624_20180704_01_T2	118/37	June 24, 2018
LC08_L1GT_118036_20190830_20190903_01_T2	118/36	Aug. 30, 2019
LC08_L1GT_118037_20190830_20190903_01_T2	118/37	Aug. 30, 2019
COMS_GOCI_L2C_GA_20140519001643	—	May 19, 2014
COMS_GOCI_L2C_GA_20150607001642	—	June 07, 2015
COMS_GOCI_L2C_GA_20160618011642	—	June 18, 2016
COMS_GOCI_L2C_GA_20170628031644	—	June 28, 2017
COMS_GOCI_L2C_GA_20180624031643	—	June 24, 2018
COMS_GOCI_L2C_GA_20190830041641	—	Aug. 30, 2019

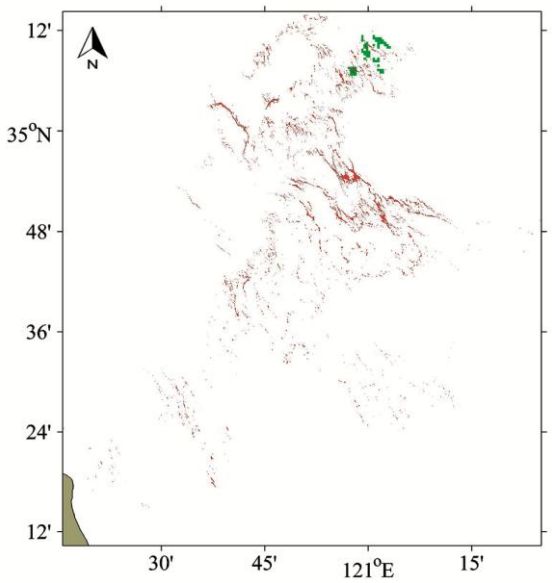

Fig. 2 — Comparison of NDVI based MABs detection between GOCI (green patches; time 00:30 UTC) and Landsat-8 (red patches; time 02:30 UTC) on May 19, 2014

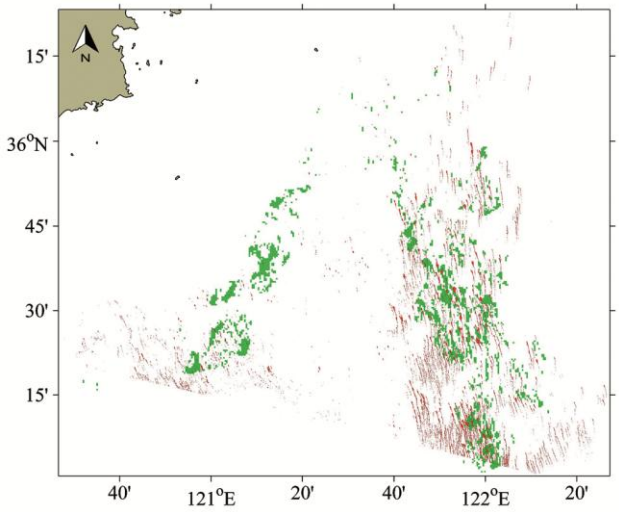

Fig. 3 — Comparison of NDVI based MABs detection between GOCI (green patches; time 00:30 UTC) and Landsat-8 (red patches; time 2:29 UTC) on June 07, 2015

Results

The present study described the findings of comparing NDVI imges between GOCI and high resolution Landsat-8. The span of dates for the satellite data were considered for six consecutive years from 2014 to 2019. On May 19, 2014 MAB occurred adjacent to the Sheyang coast and expanded on the north-east part in the YS (Fig. 2). In this figure, red coloured stripes of MAB are detected by Landsat-8 satellite; in contrast, green coloured stripes of MAB are identified by GOCI. The shape and size of MAB patches are more clear in the Landsat-8 data than that of GOCI data. The unique difference in qualities of the image is that in the GOCI image the MABs structures are quite square shaped (due to low resolution of 500 m), and in Landsat-8 the patches are sharp (due to high resolution of 30 m). Tiny stripes of MAB can be detected by Landsat-8 at a great extent. As displayed in Figure 2, MAB patches occupied about 20 km^2 in the GOCI sensor whereas about 57 km^2 area of MAB patches were detected by Landsat-8.

Massive free floating MABs are common in the summer near the offshore of Qingdao, China. In this place huge MABs were detected by the both sensors in the YS on June 07, 2015 (Fig. 3). However, two separate clusters of MAB appeared in the map. Some small patches are identified on the southeast of the map by Landsat-8 data. In contrast, GOCI sensor could not detect those parts of MAB. Similar to the

previous year Landsat-8 provided more clear image than GOCI on June 07, 2015. On the southwest of the map there are some small macroalgae stripes which are presented from the Landsat-8 data. Likewise, on the top of the map some tiny patches could not be detected effectively by GOCI sensor. Around 250 km^2 MAB on sea surface was identified by Landsat-8 sensor. On the other hand, free floating MAB of around 833 km^2 is detected by GOCI.

On June 18, 2016, MAB occurred in the center of the YS (Fig. 4). As expected, Landsat-8 sensor provided larger coverage of MABs in the mapping. However, couple of patches showed a slight shift on the northwest in the map as detected from the NDVI image of Landsat-8. On the east side, a larger area was occupied by the MAB patches. That tiny patches are detected by Landsat-8 sensor. Some areas of MAB are detected by GOCI sensor which overlapped the same macroalgae areas detected by Landsat-8. In general, it can be said that Landsat-8 is able to detect a wide area of MAB. Here, total area of MAB is estimated as 652 km^2 in the middle of the YS. Landsat-8 detected the maximum blooming area of about 388 km^2. Besides, whereas GOCI detected around 264 km^2 area in the YS.

From the NDVI image of Landsat-8 sensor, a massive MAB is detected near to the shoreline of the Qingdao on June 28, 2017 (Fig. 5). Both sensors demonstrate the similar orientations of MAB in the YS. Patches started to appear on the southwest and ended on the northeast part of the YS. Many small patches spread. Those small tiny stripes of MAB were detected by only Landsat-8 due to higher spatial resolution. Only the larger patches of MABs which were detected clearly by the GOCI sensor. Total area of MAB was 802 km^2. From Landsat-8 sensor a massive bloom was covered about 550 km^2. By GOCI, the estimated blooming area was only 251 km^2.

For drawing a clear concept of MABs occurrence, wide area was observed from Rudong to Shandong Peninsula. As a result, a large carpet-like MAB patches could be detected between offshore of Sheyang to Qingdao (Fig. 6). In this case, the wide coverage was made from the GOCI sensor. As noticed earlier, again MAB patches touched the lip of coast on June 24, 2018 at Qingdao. Also, one part of large blooms is noticed at the center of the map near to the Sheyang. However, on the southeast zone very small part of the MAB patches could be sensed by Landsat-8. On that day, Landsat-8 data was not adequate to match with the available GOCI data for the same

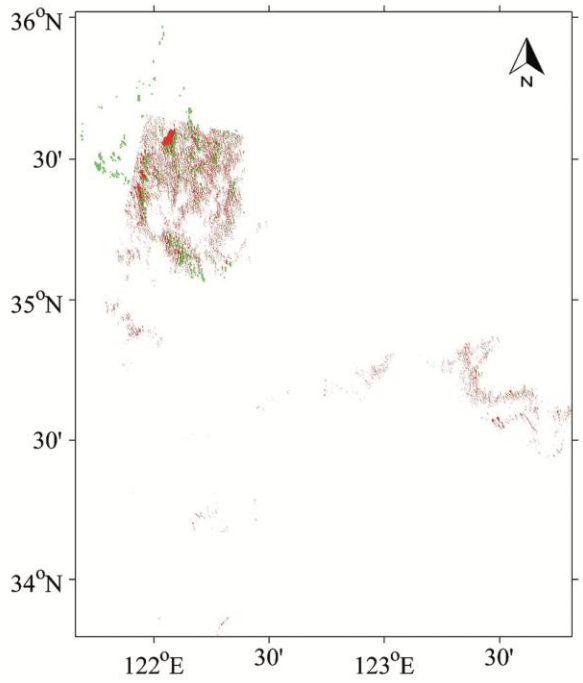

Fig. 4 — Comparison of NDVI based MABs detection between GOCI (green patches; time 01:30 UTC) and Landsat-8 (red patches; time 2:24 UTC) on June 18, 2016

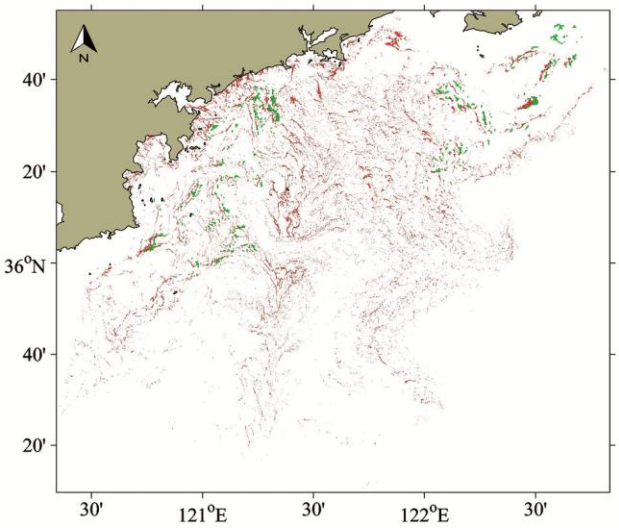

Fig. 5 — Comparison of NDVI based MABs detection between GOCI (green patches; time 03:30 UTC) and Landsat-8 (red patches; time 2:30 UTC) on June 28, 2017

place of MAB patches. On the other hand, it is noticed that some small stripes of MAB were easily detected on the southeast segment of main MAB patches by the Landsat-8. In addition, the clarity of the Landsat-8 detected MAB patches are sharper than that of the GOCI at that area. GOCI and Landsat-8 sensors managed to detect total area of around

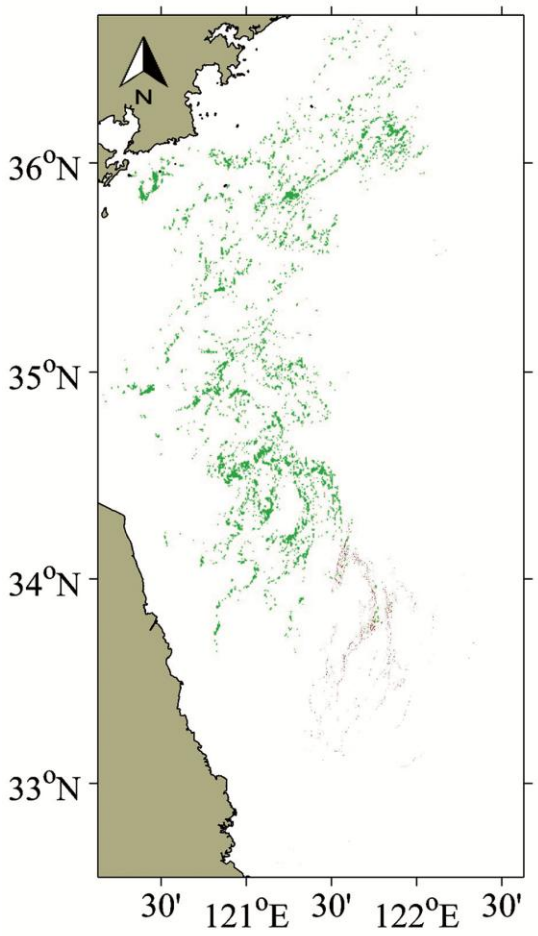

Fig. 6 — Comparison of NDVI based MABs detection between GOCI (green patches; time 03:30 UTC) and Landsat-8 (red patches; time 2:23 UTC) on June 24, 2018

2,188 km^2. Here, GOCI detected larger MAB area of 2,140 km^2. Besides, only about 48 km^2 MAB area were detected by Landsat-8. Here, two Landsat-8 images gave smaller area of MABs on June 24, 2018 because of the unavailability of Landsat-8 image data on the other paths on the same day. Eventually, The YS is fully covered by a GOCI image, but Landsat-8 images on a single path on each date can cover only a part of the YS. Thus, couple of paths are required to complete the full display of YS in terms of Landsat-8. Hence, Landsat-8 couldn't detect all MAB patches in different locations of YS in that single day due to this limitation.

In Figure 7, one of the latest observation of MAB in the YS on August 30, 2019 are presented. GOCI coverage was prominent in this area on that day. However, tiny stripes of MAB are detected by Landsat-8 on the southeast in the mapped area. Patches of MAB are located adjacent to the Sheyang.

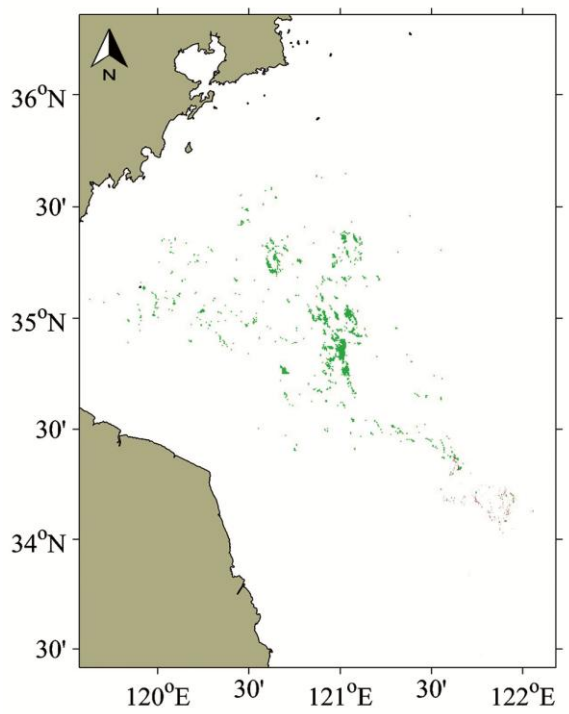

Fig. 7 — Comparison of NDVI based MABs detection between GOCI (green patches; time 04:30 UTC) and Landsat-8 (red patches; time 2:24 UTC) on August 30, 2019

Irregular forms of MAB patches are noticed in this area from GOCI sensor. MAB patches were located quite far form the coasts of Qingdao and Sheyang. MAB patches were moderate in size and covered about 492 km^2. About 10 km^2 area of MABs is detected by Landsat-8, and GOCI detected 482 km^2 MAB area. The reason for detecting less area of MAB by Landsat-8 is the same as described before in case of Figure 6.

Discussion

In this study, NDVI images are compared from both GOCI and Landsat-8. The main purpose was to find a suitable sensor for precise detection of MAB patches for taking a quick decision to avoid a large economic loss in different sectors including tourism due to sudden beaching on the coast. The MAB patches were found to spread from the middle of the YS to the offshores at Sheyang and Qingdao within six-years period of study.

MAB patches were noticed from April to July in almost every year in the YS between 2000 and 2009[refs. 24-25]. In 2008, MAB patches were detected in the Qingdao during the months of June and July[4]. Afterwards, massive blooms of *Ulva* were

documented in the same season in different parts of the YS[26-27]. In this study, MAB patches in the month of June were well observed between 2014 and 2019. Among six years of this study, the largest MAB was identified during the month of June in 2018. Unfortunately, some images could not be used in this study due to widespread dense clouds and much time difference between Landsat-8 and GOCI for those locations (Figs. 2, 6 & 7). Landsat-8 overpasses the same location in every sixteen days[28]. Thus, on the same day the satellite could not even take images of the adjacent places at the right or left paths. In contrast, in hourly intervels GOCI takes images 8 times on daily basis[29]. Such facts influence perfect matching of images to compare the status of MAB patches (Figs. 3 & 4). Therefore, some MAB patches in the YS could be detected well enough by Landsat-8 (Fig. 6). On the other hand, it is also obsereved that tiny macroalgae patches were detected accurately by Landsat-8. Besides, GOCI was able to detect only the larger patches due to having lower spatial resolution (Figs. 4 & 5). Generally, Landsat-8 detected smaller patches of MAB which will provide extra advantage to take control measure for avoiding a huge damage to the beach environment. Therefore, NDVI image from Landsat-8 give advantages for indentifying MAB at the early stage of proliferation of macroalgae.

Conclusion

Multi-sensor detection is quite common in different regions of the world. However, in the YS two popular satellite sensors, Landsat-8 and GOCI, were used to detect MABs. The performance of Landsat-8 was appreciable with NDVI images to identify the MABs. MABs identification was made in May, June or August in different years of the study period. Generally, MABs were found near the coast of Sheyang and Qingdao, within these six years. The largest MAB was detected by both Landsat-8 and GOCI sensors along the coast of Sheyang and Qingdao in 2018. The locations of MABs were almost adjacent areas during the development phase of MAB. Here, the range of MABs were in between the cental YS to the coast of Sheyang and Qingdao. The advantage of the GOCI is to get image data at any date all the year round, but images were of low spatial resolution. In case of Landsat-8, their spatial resolution is quite high and quality of image is sharp enough, but it could not able to provide data everyday for each path; therefore, the temporal coverage is much smaller than GOCI. Moreover, coverage of each image's for Landsat-8 is much smaller than that of the GOCI. This is another key reason to get smaller coverage of MAB from Landsat-8.

Acknowledgements

The authors are profoundly delighted to acknowledge the Korea Institute of Ocean Science & Technology (KIOST) and United States Geological Survey (USGS) for providing access to GOCI and Landsat 8 data, respectively, to complete the research. They do also extend their heartiest thanks to all the reviewers for their sound review in improving this manuscript. This research is part of the projects entitled "Monitoring System of Spilled Oils Using Multiple Remote Sensing Techniques", funded by the Korea Coast Guard.

Conflict of Interest

The authors declare there are no conflicts of interest.

Author Contributions

Conceptualization, methodology, data procurement, analysis and writing: MHS; analysis, writing, review and editing: AHAR; and conceptualization, review, editing and overall supervision: CSY.

References

1 Nelson T, Nelson A & Tjoelker M, Seasonal and spatial patterns of "green tides" (ulvoid algal blooms) and related water quality parameters in the coastal waters of Washington State, USA, *Bot Mar, 46 (*2003) 263–275.

2 Yabe T, Ishii Y, Amano Y, Koga T, Hayashi S, *et al*., Green tide formed by free-floating *Ulva* spp. at Yatsu tidal flat, Japan, *Limnology, 10 (*2009) 239–245.

3 Dhargalkar V K, Untawale A G & Jagtap T G, Marine macroalgal diversity along the Maharashtra coast: Past and present status, *Indian J Geo-Mar Sci*, 30 (2001) 18-24.

4 Keesing J K, Liu D, Fearns P & Garcia R, Inter- and intra-annual patterns of *Ulva prolifera* green tides in theYellow Sea during 2007–2009, their origin and relationship to the expansion of coastal seaweed aquaculturein China, *Mar Pollut Bull, 62 (*2011) 1169–1182.

5 Liu H, Liu X & Jiang A, Seasonal changes of macroalgal composition, biomass and assemblage diversity in the rocky intertidals of Zhifu Tombolo, China, *Indian J Geo-Mar Sci*, 46 (2017) 1091–1097.

6 Liu D & Zhou M, Green Tides of the Yellow Sea: Massive Free-Floating Blooms of *Ulva prolifera*, In: *Global Ecology and Oceanography of Harmful Algal Blooms*, eduted by P Glibert, E Berdalet, M Burford, G Pitcher & M Zhou, (Springer, Cham, Switzerland), 2018, pp. 317-326.

7 Morand P & Briand X, Excessive growth of macroalgae: A symptom of environmental disturbance, *Bot Mar, 39* (1996) 491–516.

8 Teichberg M, Fox S E, Olsen Y S, Valiela I, Martinetto P, *et al*., Eutrophication and macroalgal blooms in temperate

and tropicalcoastal waters: Nutrient enrichment experiments with *Ulva* spp., *Global Change Biol*, *16 (*2010) 2624–2637.

9 Ye N H, Zhang X W, Mao Y Z, Liang C W, Xu D, *et al*., 'Green tides' are overwhelming the coastline of our blue planet: Taking the world's largest example, *Ecol Res*, *26* (2011) 477–485.

10 Zhang X, Xu D, Mao Y, Li Y, Xue S, *et al*., Settlement of vegetative fragments of *Ulva prolifera* confirmed as an important seed source for succession of a large-scalegreen tide bloom, *Limnol Oceanogr*, *56* (2011) 233–242.

11 Lee J H, Pang I C, Moon I J & Ryu J H, On Physical Factors that Controlled the Massive Green Tide Occurrence along the Southern Coast of the Shandong Peninsula in 2008: A Numerical Study Using A Particle-Tracking Experiment, J Geophys Res, 116 (2011) 1–12.

12 Liu D, Keesing J K, Xing Q & Shi P, World's Largest Macroalgal Bloom Caused by Expansion of Seaweed Aquaculture in China, Mar Pollut Bull, 58 (2009) 888–895.

13 Xu Q, Zhang H & Cheng Y, Multi-Sensor Monitoring of Ulva prolifera Blooms in theYellow Sea Using Different Methods, Front Earth Sci, 10 (2016) 378–388.

14 Hu C M & He M X, Origin and Offshore Extent of Floating Algae in Olympic Sailing Area, *EOS Tran Am Geophys Un*, 89 (2008) 302–303.

15 Xu Q, Zhang H, Cheng Y, Zhang S & Zhang W, Monitoring and Tracking the Green Tide in the Yellow Sea with Satellite Imagery and Trajectory Model, IEEE J Sel Top App Earth Obs, 9 (2016) 5172–5181.

16 Harun-Al-Rashid A & Yang C S, Hourly variation of green tide in the Yellow Sea during summer 2015 and 2016 using Geostationary Ocean Color Imager data, *Int J Remote Sens*, 39 (2018) 4402–4415.

17 Xing Q & Hu C, Mapping macroalgal blooms in the Yellow Sea and East China Sea using HJ-1 and Landsatdata: Application of a virtual baseline reflectance height technique, *Remote Sens Environ*, *178* (2016) 113–126.

18 Shi W & Wang M, Green Macroalgae Blooms in the Yellow Sea during the Spring and Summer of 2008, *J Geophys Res*, 114 (2009) 1–10.

19 Yu H, Lee J Y, Lee W K, Cui G, Cho J K, *et al*., Application of CASI Hyperspectral Image to Analysis of the Distribution of Hydrogen-Fluoride-Damaged Vegetation in Gumi, Korea, *J Indian Soc Remote*, 45 (2016) 317–326.

20 Yang C S & Song J H, Geometric Performance Evaluation of the Geostationary Ocean Color Imager, *Ocean Sci J*, 47 (2012) 235–246.

21 KOSC, GOCI L2 (Ver. 2.0) Rayleigh Corrected Reflectance., http://kosc.kiost.ac.kr/eng/p10/kosc_p11.html (9/2019).

22 United States Geological Survey, Landsat collection 1. Earth Explorer.https://earthexplorer.usgs.gov (9/2019).

23 RBINS, ACOLITE. https://odnature.naturalsciences.be/remsem/software-and data/acolite (2/2018).

24 Hu C, Li D, Chen C, Ge J, Muller-Karger F E, *et al*., On the recurrent Ulva prolifera blooms in the Yellow Sea and East China Sea, *J Geophys Res*, 115 (2010) 1–8.

25 Liu D, Keesing J K, Xing Q & Shi P, World's largest macroalgal bloom caused by expansion of seaweed aquaculture in China, *Mar Pollut Bull*, 58 (2009) 888–895.

26 Huo Y, Zhang J, Chen L, Hu M, Yu K, *et al*., Green algae blooms caused by *Ulva prolifera* in the southern Yellow Sea: Identification of the original bloom location and evaluation of biological processes occurring during the early northward floating period, *Limnol Oceanogr*, 58 (2013) 2206–2218.

27 Xing Q, Hu C, Tang D, Tian L, Tang S, *et al*., World's Largest Macroalgal Blooms Altered Phytoplankton Biomass in Summer in the Yellow Sea: Satellite Observations, *Remote Sens*, 7 (2015) 12297–12313.

28 Roy D P, Wulder M A, Loveland T R, Woodcock C E, Allen R G, *et al*., Landsat-8: Science and product vision for terrestrial global change research, *Remote Sens Environ*, 145 (2014) 154–172.

29 Ryu J H, Han H J, Cho S, Park Y J & Ahn Y H, Overview of Geostationary Ocean Color Imager (GOCI) and GOCI Data Processing System (GDPS), *Ocean Sci J*, 47 (2012) 223–233.